Katharina Breunig, Ingo Spahn*, Alex Hermanne, Stefan Spellerberg, Bernhard Scholten and Heinz H. Coenen

Cross section measurements of $^{75}As(\alpha,xn)^{76,77,78}Br$ and $^{75}As(\alpha,x)^{74}As$ nuclear reactions using the monitor radionuclides ^{67}Ga and ^{66}Ga for beam evaluation

DOI 10.1515/ract-2016-2593
Received February 24, 2016; accepted November 10, 2016

Abstract: For the production of the medically interesting radionuclides ^{76}Br and ^{77}Br cross sections of α-particle induced reactions on arsenic, leading to the formation of $^{76,77,78}Br$ as well as to the non-isotopic impurity ^{74}As, were measured from their thresholds up to 37 MeV. Sediments of elemental arsenic were used as targets and irradiated, using the established stacked-foil technique. In order to remove discrepancies of the existing literature data, the cross section ratios of the monitor nuclides $^{67}Ga/^{66}Ga$ were used for determination of the α-particle energies as well as the effective beam current through all the stacks, thus inferring the experimental cross sections. Compared with the available excitation functions the new data indicate slightly divergent curve shapes. In the case of ^{76}Br the excitation function seems to be shifted to somewhat lower α-particle energies, and also the maximum cross section of the formation of ^{77}Br tends to be slightly lower compared with the curve recommended to date. In the case of a re-evaluation, these new data should be taken into account, as they may contribute to enhance the accuracy of the excitation functions.

Keywords: α-particles, radiobromine, radioarsenic, cross sections, integral yield, monitor reactions.

***Correspondence author: Ingo Spahn,** Institute for Neuroscience and Medicine, INM-5: Nuclear Chemistry, Forschungszentrum Jülich, Jülich, Germany, E-mail: i.spahn@fz-juelich.de
Katharina Breunig, Stefan Spellerberg, Bernhard Scholten and Heinz H. Coenen: Institute for Neuroscience and Medicine, INM-5: Nuclear Chemistry, Forschungszentrum Jülich, Jülich, Germany
Alex Hermanne: Cyclotron Laboratory, Vrije Universiteit Brussel (VUB), Brussels, Belgium

1 Introduction

Radiobromine is of special interest for labelling of tracer molecules, because there are isotopes available which are suitable for both molecular imaging approaches and radiotherapy (*cf.* [1–3]). In addition, bromine is a versatile element concerning its chemistry of labelling, as the same methods developed for radioiodine can in principle be used or adapted (for early reviews cf. [4, 5]). The neutron deficient isotope ^{76}Br, with a half-life of 16.2 h and a β^+-branching of 58.2% [6] ($\beta^+_{max} = 3.4$ MeV; stable daughter ^{76}Se) lends itself as potential longer-lived "non-standard" PET nuclide for imaging of slow metabolic processes, or those with slow clearance of non-specific binding [7], as well as for drug development purposes. The rather high end-point energy of the emitted positrons and several high-energy γ-rays ($E_\gamma > 500$ keV, see Table 1) lead to some limitations, concerning spatial resolution and image quality [7, 9], but may be reduced by appropriate specific corrections in the image reconstruction [9]. Furthermore, the advancing techniques of hybrid imaging using PET/MR devices may reduce these limitations as the positron range will be reduced under the influence of strong magnetic fields [10, 11].

The other neutron deficient isotope ^{77}Br decays almost exclusively via electron capture (99.3%) to its stable daughter ^{77}Se. The emitted Auger electrons as well as the convenient and suitable half-life of 57 h make it an attractive nuclide for internal radiotherapy. Due to the emitted 239 keV γ-ray ($I_\gamma = 23\%$) ^{77}Br is additionally suited for SPECT, hence representing a so called theragnostic radionuclide. Thus, the quantitation and dosimetry of ^{77}Br-labelled radiotherapeutical agents might be accomplished using the original compound, ensuring authentic *in vivo* behavior.

Natural arsenic (100% ^{75}As) has been used for producing ^{76}Br and ^{77}Br in radionuclidically pure form, using ^3He- and α-particle induced reactions (for early reviews

Table 1: Relevant decay data of investigated radionuclides [8].

Radionuclide	$T_{1/2}$	Analyzed γ-rays [keV] (% branching)	
^{76}Br	16.2 h	559.090	(74)
		657.020	(15.9)
		1853.670	(14.7)
^{77}Br	57.04 h	238.980	(23.1)
		297.230	(4.16)
^{78}Br	6.45 min	613.680	(13.6)
^{74}As	17.77 days	595.830	(59)

cf. [12, 13]). This has a big advantage over proton or deuteron bombardment of selenium targets, since no costly enriched target material is necessary. Experimental cross section data of the nuclear reactions ^{75}As(α,3n)^{76}Br and ^{75}As(α,2n)^{77}Br were measured by several groups, and were recently evaluated by Aslam et al. [14] and Hassan and Qaim [15], respectively. However, the different data sets show quite strong deviations.

In order to improve the existing data, reaction cross sections of α-particle induced reactions on arsenic, leading to the formation of ^{76,77,78}Br and ^{74}As, were measured in this work from their threshold up to 37 MeV. An improvement of the experimental data was aimed at by using the ratios of the monitor nuclides ^{67}Ga and ^{66}Ga, both generated by (α,*x*)-reactions on ^{nat}Cu. This allowed the simultaneous determination of the α-particle energies independently from the particle flux and under the given experimental conditions.

2 Experimental

2.1 Materials

Elemental arsenic powder of high purity (99.999%, Sigma-Aldrich, USA) was used as target material. For energy degradation or beam monitoring aluminum (99%), copper (99.9%) and titanium (99.96%) foils, purchased from Goodfellow Ltd., England, were used. The aluminum foils were also applied as backing material.

2.2 Sample preparation

Thin samples for irradiation were prepared by sedimentation of elemental arsenic powder onto aluminum backings of 25 μm thickness out of a suspension of ethanol. The targets consisted of 5–11 mg/cm^2 arsenic and were additionally covered by a 10 μm thick aluminum foil for protection, resulting in an Al-As-Al sandwich geometry.

2.3 Irradiations and beam monitoring

For the measurement of reaction cross sections the prepared Al-As-Al sandwiches were irradiated in stacked-foil arrangements, together with aluminum foils as degraders and copper and titanium foils for beam monitoring. In total, 30 stacks consisting of 1–4 arsenic targets were irradiated at the CGR-560 of the Vrije Universiteit Brussel (VUB) in Brussels, Belgium, with 38 MeV α-particles and a beam current of about 70 nA. For measurement of the longer lived radionuclides ^{76,77}Br and ^{74}As an irradiation time of 30 min was chosen; and for the short-lived ^{78}Br a beam time of 6 min. For planning of the individual stacks, the energy degradation of the α-particle beam was calculated using the in-house computer code STACK. This code is based on an iterative formalism of the Bethe equation, modified by Williamson et al. [16] and implemented in an EXCEL matrix.

The beam current of each irradiation was measured with a Faraday cup as well as using the well-known monitor reactions ^{nat}Cu(α,*x*)^{66,67}Ga and ^{45}Ti(α,*x*)^{51}Cr [17]. At energies above 10 MeV copper foils were inserted into the stack, while titanium foils were used at energies below 10 MeV. One monitor foil was placed in front of the target holder, directly hit by the particle beam. Additionally, one copper foil was placed in front of each target and one at the end of the stack.

When comparing the cross sections of the above mentioned monitor reactions obtained by using the beam current measured with the Faraday cup and taking the initial STACK energies into account, significant deviations from the literature data were observed. As known from the literature [18, 19] the energy of an incident particle can be described as a function of the ratio of two radionuclides, generated in the same monitor foil [8]. Following this, the energies of the α-particles were corrected by using the ratios of the generated radioactivity of the monitor nuclides ^{67}Ga and ^{66}Ga. This quotient is not dependent on the beam current, but exclusively on the projectile energy. Independent of the α-particle energy, the ratios of the ^{67}Ga and ^{66}Ga cross sections, taken from [17], were calculated. The initial STACK energies were revised accordingly, and consequently the beam current in each monitor foil was calculated, using those corrected α-energies.

2.4 Measurement of radioactivity

All generated radioactivity was measured by γ-ray spectrometry using well-calibrated HPGe detectors of EG & G Ortec, USA, and Canberra Industries Inc., USA. All targets and monitor foils were measured non-destructively. To minimize coincidence summing, all measurements were performed at sample-to-detector distances of at least 10 cm. Additionally, for prevention of pile-up pulses, detector dead times of more than 10% were avoided. The investigated radionuclides were identified by their characteristic γ-rays (see Table 1), using the software *GammaVision 6.01* (EG & G Ortec) and *Genie2000* (Canberra Industries Inc.).

2.5 Calculation of reaction cross sections and integral yields

Reaction cross sections were calculated from the measured radioactivity, the particle flux and the number of target nuclei using the well-known activation formula. The radioactivity was corrected for decay during the counting period as well as for decay after the end of bombardment (EOB). All cross sections were measured cumulatively upon the decay of the metastable states ^{76m}Br ($T_{1/2}$ = 1.32 s) and ^{77m}Br ($T_{1/2}$ = 4.3 min), respectively.

Integral thick target yields were calculated by adding up the corresponding differential yields in the considered energy range. Here, the differential yields of radionuclides were determined from the measured cross sections in energy intervals of 1 MeV by using the activation formula as well. The required target masses, leading to an energy degradation of exactly 1 MeV, were calculated with the computer code STACK.

2.6 Consideration of uncertainties

The overall uncertainties of the reaction cross sections were calculated from the contribution of the respective individual uncertainties according to the Gaussian error propagation. That way, cross section uncertainties of 6–13% were determined, resulting from the uncertainties of the target mass (0.3–1.3%), detector efficiency (4–6%), decay data (0.01–5%), peak area analysis (0.1–8%) and the particle flux (5–7%).

The uncertainties of the yields of radionuclides added up to 8–10%. Their maximum uncertainty was somewhat lower than the maximum uncertainty of the cross section data, because for the calculation of the uncertainties of the yields the average uncertainty of the measured cross sections was multiplied by that of the single cross sections. Those were determined by the interpolated excitation function for calculating the differential yields (see Chapter 2.5).

The uncertainties of the projectile energies were determined from the average energy loss of the α-particle beam in the considered target. The respective entry energy of the beam was deduced form the ratio of the monitor radionuclides as described in Section 2.3. Because of the high linear energy transfer (LET) of the α-particles, the overall uncertainties were quite high and increased rapidly with progressing energy degradation. In the energy range 38 → 20 MeV uncertainties of 2–9% were found, in the energy range 20 → 15 MeV, 6–12%, and for the energy range 15 → 9 MeV, 7–19%.

3 Results and discussion

3.1 Correction of particle energies

When using the STACK energies and the individual beam currents measured with the integrator, significant deviations were observed, comparing the here experimentally determined cross sections of the used monitor reactions with the corresponding literature data. Thus, the projectile energies and consequently also the beam currents were corrected by taking the ratio of the monitor nuclides ^{67}Ga and ^{66}Ga into account. As an example Figure 1 shows

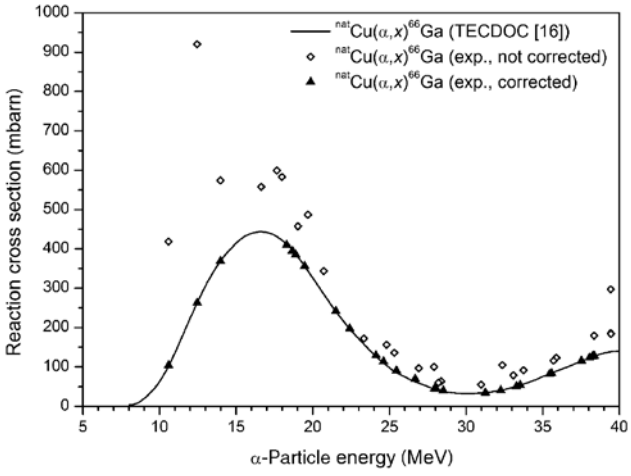

Figure 1: Experimental cross sections of the monitor reaction ^{nat}Cu(α,x)^{66}Ga with and without correction in comparison to the recommended excitation function [17].

the substantial influence of this revision regarding the monitor reaction $^{nat}Cu(\alpha,x)^{66}Ga$.

The cross sections obtained, using the STACK energies and the integrator flux, obviously deviate strongly from the recommended data [17]. Due to the fact that Figure 1 pictures a series of experiments, the degree of deviation across the investigated energy range is not homogeneous. A monitor foil placed in front of each arsenic sample allowed the determination of the "true" α-particle energy and effective beam current at each target sample during the irradiations. After energy and flux correction based on the $^{67}Ga/^{66}Ga$ ratios, our data show an excellent agreement with this evaluated excitation function.

3.2 Reaction cross section data

The experimentally determined cross section data of the nuclear reactions $^{75}As(\alpha,xn)^{76,77}Br$ and $^{75}As(\alpha,x)^{74}As$ together with their respective uncertainties are given in Table 2. The data of the $^{75}As(\alpha,n)^{78}Br$ nuclear reaction were determined in individual irradiation experiments and are listed separately in Table 3.

Each reaction is dicussed below individually.

$^{75}As(\alpha,3n)^{76}Br$: The measured cross sections of the $^{75}As(\alpha,3n)^{76}Br$ nuclear reaction are graphically shown in Figure 2 in dependence of the α-particle energy up to 50 MeV, together with the literature data [20–23], including both the TENDL-2014 and TENDL-2015 data [24, 25] as well as the evaluated excitation function of Aslam et al. [14]. Limited by the incident α-particle energy of the CGR-560 cyclotron, the increase of the $^{75}As(\alpha,3n)^{76}Br$ excitation function (E_{thr} = 25.8 MeV) could only be covered up to 37 MeV, where a cross section of 478 mbarn was found.

In general the different data sets deviate slightly from each other. The experimental results measured in this work support the two data points of Nozaki et al. [20], while showing an energy shift to lower α-particle energies when compared with the cross sections reported by Alfassi and Weinreich [21]. Since the data of Paans et al. [22] cover the energy range above 37 MeV, a comparison with our lower-energy data cannot be done. With regard to the cross sections of Hermanne et al. [23] our values show about 1 MeV shift to lower energies, i. e. much less pronounced than that from the data by Alfassi and Weinreich [21].

All literature data were evaluated in 2011 by Aslam et al. [14] by using different computer codes. Based on the experimental and the theoretical results, but excluding the data point of Nozaki et al. at 35 MeV as well as the cross sections given by Alfassi and Weinreich below 55 MeV, which did not meet the criteria set for evaluation, Aslam et al. recommend the excitation function shown in Figure 2. Thus, their recommended curve primarily represents the cross sections of Hermanne et al. [23] and Paans et al. [22], indicating a maximum of about 390 mbarn at 40 MeV. A possible reason for the deviation of the older data may be the use of different cross section data for the beam monitoring at that time.

The experimental data obtained in this work, however, suggest that the $^{75}As(\alpha,3n)^{76}Br$ reaction has a higher maximum with cross sections of at least 478 mbarn at a possibly somewhat lower α-particle energy around 37 MeV. The TENDL data appear to support this conclusion; however, the overall agreement with the experimental

Table 2: Measured cross sections of the nuclear reactions $^{75}As(\alpha, 3n)^{76}Br$, $^{75}As(\alpha, 2n)^{77}Br$ and $^{75}As(\alpha, x)^{74}As$.

E_α [MeV]	Cross section (mb)		
	$^{75}As(\alpha, 3n)^{76}Br$	$^{75}As(\alpha, 2n)^{77}Br$	$^{75}As(\alpha, x)^{74}As$
13.6 ± 1.8	–	19.0 ± 1.2	–
15.9 ± 1.2	–	151 ± 14	–
16.3 ± 1.0	–	192 ± 16	0.12 ± 0.01
17.8 ± 2.0	–	285 ± 23	0.5 ± 0.1
17.9 ± 1.1	–	374 ± 32	0.5 ± 0.1
18.5 ± 1.9	–	497 ± 42	2.2 ± 0.2
19.5 ± 1.2	–	508 ± 38	5.6 ± 0.6
20.3 ± 1.8	–	572 ± 50	8.5 ± 0.9
21.0 ± 1.1	–	582 ± 52	11.7 ± 1.2
21.2 ± 1.3	–	580 ± 48	6.0 ± 0.6
21.7 ± 1.8	–	813 ± 68	22.3 ± 2.3
22.0 ± 1.3	–	612 ± 48	8.8 ± 0.9
22.2 ± 0.7	–	568 ± 48	6.9 ± 0.7
22.3 ± 1.1	–	591 ± 50	9.9 ± 0.9
22.7 ± 0.9	–	615 ± 53	17.0 ± 1.6
23.4 ± 1.4	–	750 ± 63	23.6 ± 2.3
24.6 ± 1.1	–	707 ± 60	36.6 ± 3.5
25.4 ± 1.5	–	811 ± 63	49.0 ± 4.8
26.0 ± 0.8	0.7 ± 0.1	637 ± 54	35.2 ± 3.3
26.4 ± 1.3	31.0 ± 3.0	694 ± 64	53.4 ± 5.4
26.6 ± 1.1	13.7 ± 1.1	668 ± 55	48.8 ± 4.5
27.1 ± 1.6	62.1 ± 4.9	687 ± 51	68.6 ± 6.3
28.4 ± 1.5	52.8 ± 4.4	680 ± 56	69.8 ± 7.0
29.2 ± 1.2	72.2 ± 5.8	567 ± 45	58.5 ± 5.2
29.8 ± 0.9	165 ± 14	635 ± 56	82.7 ± 8.0
31.0 ± 0.8	191 ± 15	572 ± 50	88.2 ± 8.2
31.3 ± 1.3	208 ± 20	464 ± 42	69.9 ± 7.0
31.8 ± 1.1	300 ± 23	534 ± 43	98.9 ± 8.8
33.7 ± 0.8	291 ± 24	342 ± 29	74.1 ± 6.9
34.9 ± 0.8	421 ± 41	296 ± 27	81.9 ± 8.2
35.1 ± 0.8	391 ± 31	316 ± 27	88.3 ± 8.4
35.7 ± 0.9	410 ± 33	211 ± 18	70.4 ± 6.6
36.9 ± 0.5	419 ± 33	165 ± 14	71.4 ± 6.6
36.9 ± 0.7	478 ± 38	181 ± 15	87.6 ± 8.2

Table 3: Measured cross sections of the nuclear reaction $^{75}As(\alpha,n)^{78}Br$.

E_α [MeV]	Cross section (mb)
8.8 ± 1.7	86 ± 7
9.9 ± 1.6	117 ± 10
11.2 ± 1.7	243 ± 21
11.5 ± 1.4	287 ± 23
13.0 ± 1.5	368 ± 27
13.1 ± 2.1	347 ± 29
14.3 ± 1.0	364 ± 30
14.6 ± 2.0	468 ± 39
14.9 ± 1.6	439 ± 36
15.2 ± 1.2	422 ± 33
15.7 ± 1.9	371 ± 28
16.3 ± 1.1	382 ± 32
17.3 ± 1.4	339 ± 27
18.0 ± 1.8	182 ± 14
18.2 ± 1.7	261 ± 20
18.9 ± 1.3	147 ± 12
19.1 ± 1.1	188 ± 15
20.3 ± 1.4	134 ± 11
21.1 ± 1.5	118 ± 9
23.4 ± 1.5	65.0 ± 5.6
24.4 ± 1.4	42.4 ± 3.3
27.1 ± 1.4	27.6 ± 2.2
28.4 ± 1.3	26.0 ± 2.3
29.6 ± 1.7	22.9 ± 1.8
32.6 ± 1.3	14.6 ± 1.2
34.2 ± 1.7	9.1 ± 0.8
35.3 ± 1.6	8.2 ± 0.8
37.9 ± 0.7	8.8 ± 1.0

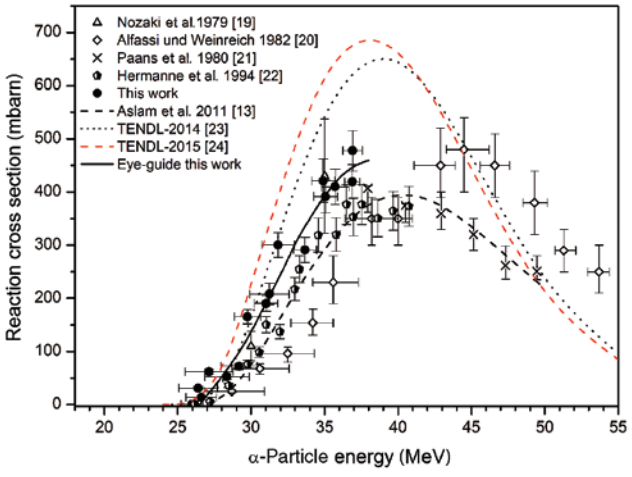

Figure 2: Experimental cross sections of the nuclear reaction $^{75}As(\alpha,3n)^{76}Br$ together with the data from literature [20–24] and the evaluated excitation function [14].

data is rather poor. To describe the whole excitation function, irradiations with at least 50–55 MeV α-particles are necessary. However, cyclotrons providing α-particles of such higher energies are extremely rare, and in addition to that, the longer-lived isotope ^{77}Br is always co-produced *via* the $^{75}As(\alpha,2n)$-process. Consequently, the α-particle induced production of ^{76}Br would generally be inferior to, e. g. the $^{76}Se(p,n)$-reaction [25, 26].

$^{75}As(\alpha,2n)^{77}Br$: The experimental cross sections of the $^{75}As(\alpha,2n)$-reaction (E_{thr} = 14.2 MeV) leading to the formation of ^{77}Br are depicted in Figure 3 together with the available literature data and the evaluated excitation function given by Hassan and Qaim [15], considering the relevant energy range of 10 to 40 MeV. Around the maximum at about 25 MeV the new data indicate cross sections of about 700 mbarn.

Concerning the general trend, the cross sections of all experiments show a rather good agreement, in principle. However, there are clear discrepancies in the height of the maximum. Above 18 MeV the cross sections found in our work agree well with those of Waters et al. [27], but tend to be somewhat smaller, or alternatively have higher particle energies as a consequence of an energy shift in the lower energy region. Compared to the data of Nozaki et al. [20] the new ones indicate significantly lower cross sections, but show excellent agreement with those of Alfassi and Weinreich [21]. Qaim et al. [28] report higher cross sections at α-particle energies above 20 MeV with values up to 850 mbarn at about 23 MeV, implying a shift of the maximum downwards by about 2 MeV. This is also observed in the case of the $^{75}As(\alpha,n)^{78}Br$ reaction (see Figure 3). So this shift is real. The data of Hermanne et al. [23] agree well, concerning the position of the maximum, but show about 15 to 20% lower values of cross sections.

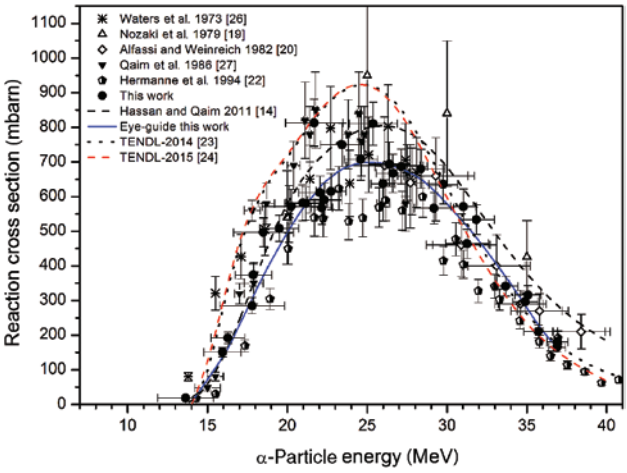

Figure 3: Experimental cross sections of the nuclear reaction $^{75}As(\alpha,2n)^{77}Br$ together with the data from literature [20, 21, 23, 24, 27, 28] and the evaluated excitation function [15].

This is comparable to the deviation found in case of the (α,3n)-reaction discussed above and is most likely due to the same reason.

The dashed line in Figure 3 represents the excitation function recommended by Hassan and Qaim [15] from their evaluation based on the experimental data published until 2011, but not considering those of Hermanne et al. [23]. This recommended curve indicates a maximum of about 800 mbarn at 26 MeV. In view of the new cross section data, however, a somewhat lower and narrower maximum seems more probable.

In contradiction to the experimental results the theoretical cross section data provided by the TENDL-2014 and TENDL-2015 data sets [24, 25] support a broader excitation function with higher maximum. It is noticable that the two TENDL curves disagree rather significantly. Wheras TEND-2015 agrees better with the experimental data in the higher energy range, the agreement in the lower energy range apears to be worse than the 2014 data.

^{75}As(α,n)^{78}Br: In Figure 4 the measured cross sections leading to the formation of the short-lived isotope ^{78}Br *via* the ^{75}As(α,n)-process are shown in dependence of the α-particle energy and in comparison with the literature data of Qaim et al. [28] and Hermanne et al. [23]. The experimental values determined in this work indicate a maximum at 15 MeV with cross sections of more than 400 mbarn.

The new data show significant deviations from the values of Qaim et al. [28]. The maximum of our excitation function is considerably broader and shifted to lower α-particle energies by ca. 3 MeV. The shape of the computer modeled TENDL curves, shown as dotted lines in the figure, also indicate such a shift, and generally agree rather well with our experimental data, except that the peak is narrower and the maximum cross section values appear to be overestimated by the code. As mentioned in the experimental section, in this work all γ-ray measurements could be done non-destructively, because aluminum was used as backing material, which is hardly activated by α-particles. In contrast, Qaim et al. [28] used copper backings, where ^{nat}Cu(α,*x*)-reactions cause high background radioactivity, resulting from different gallium isotopes. In that study, the electroplated arsenic could not be removed completely quickly from the copper matrix and only the ratio of ^{78}Br and ^{77}Br was measured in the solution. Then the percentage of dissolved radiobromine was determined indirectly by measurement of the radioactivity of the longer lived ^{77}Br remaining on the backing. That correction factor was then applied to the activity of ^{78}Br. This is a standard radiochemical technique but the correction may be high. The observed energy shift of the new data can be related most likely to the fact that the nominal incident projectile energy of 28 MeV of the employed cyclotron CV28 assumed in the earlier study in 1986 was too high. Kormány published a measured value of only 26.799 MeV in 1994, determined by a new non-interfering experimental method [29]. Due to the high LET of α-particles this deviation of 1.2 MeV would strongly accumulate with increasing energy degradation, matching the observed bias of energy in Figure 4. The new cross sections measured in this work show good agreement above 15 MeV with those by Hermanne et al. [23]. It is interesting to report that in later years Sudár and Qaim measured the excitation functions of the ^{55}Mn(α,n)^{58m,g}Co reactions [30, 31] using the corrected 26.8 MeV as incident α-particle energy and got results in good agreement with other experimental data and nuclear model calculations.

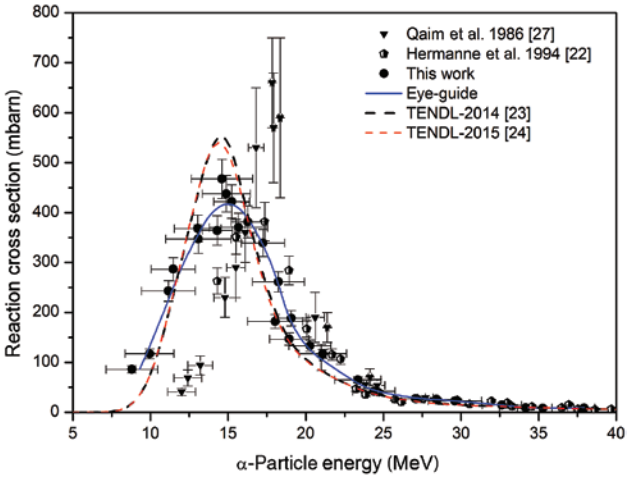

Figure 4: Experimental cross sections of the nuclear reaction ^{75}As(α,n)^{78}Br together with the data from literature [23, 24, 28].

^{75}As(α,x)^{74}As: The experimental cross sections of the ^{75}As(α,*x*)-process leading to the formation of the non-isotopic radioactive by-product ^{74}As are depicted in Figure 5. Here, maximum cross sections of about 86 mbarn were measured at α-particle energies of about 33 MeV. In the energy range below 30 MeV the prevalent process is probably the ^{74}As(α,αn)-reaction (E_{thr} = 10.8 MeV), whereas above 30 MeV several reaction channels, e. g. ^{75}As(α,t + d)-, ^{75}As(α,^{3}He + 2n)- or ^{75}As(α,2p + 3n)-process (E_{thr} = 29.3 MeV, E_{thr} = 32.5 MeV and E_{thr} = 40.6 MeV, respectively) may start contributing to the excitation function. The new data agree well with the earlier cross sections of Levkovskij [32] from 1991. However, since he did not give any experimental details or uncertainties concerning the results, the new cross sections for the ^{75}As(α,x)^{74}As reaction represent

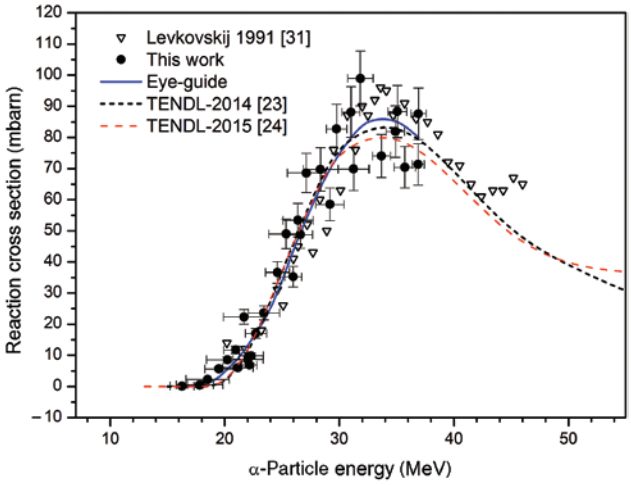

Figure 5: Experimental cross sections of the nuclear reaction $^{75}As(\alpha,x)^{74}As$ together with the data from literature [24, 32].

the first authentic and reproducible values. The comparison with the TENDL data taken from the literature [24, 25] shows a remarkably good agreement in both the shape and the intensity of the excitation function.

Summarizing, the results of the reaction cross section data lead to following observations: Nozaki et al. [20] and Paans et al. [22] did not report uncertainties for the α-particle energies at all, and the cross section uncertainties of Nozaki et al. are given as generally 25% which seems to be only an estimated value. The uncertainties of the α-particle energies in Figures 2 and 3 given by Alfassi and Weinreich [21] also seem to be estimations. They used an incident α-particle energy of about 100 MeV at the cyclotron JULIC and the beam was degraded in the stack to energies down to 30 MeV. Hermanne et al. [23] indicate the projectile energies uncertainties within a range of 0.6–1 MeV, and the uncertainties of the experimental cross sections were given in general as 10%, considering the appropriate contributing factors independent of the projectile energy.

In contrast to all publications, in this work the α-particle energies were determined as outlined above by using the ratios of the monitor nuclides $^{67}Ga/^{66}Ga$ which was more suitable due to the high LET of α-particles. Thus, the observed deviations from the literature data probably result from an energy shift related to this energy correction. Differences in the height of the maximum of several nuclear reactions, e. g. in Figures 2 and 3, may possibly be explained by the adjustment of the particle flux as a consequence of the energy correction as well.

Regarding the cross section data obtained from the TENDL-2014 and TENDL-2015 data files, the agreement with the experimental data is quite good in case of the $^{75}As(\alpha,n)^{78}Br$ and $^{75}As(\alpha,x)^{74}As$ reactions, but it is rather poor in case of the $^{75}As(\alpha,3n)$- and the $^{75}As(\alpha,2n)$- process.

3.3 Integral yields of resulting radionuclides from α-bombardment of arsenic

Integral radionuclide production yields of the bromine radioisotopes ^{76}Br, ^{77}Br and ^{78}Br as well as the non-isotopic by-product ^{74}As were determined based on the new cross section data determined in this work. Calculations were done using the eye-guides shown in Figures 2–5 and are illustrated in Figure 6 in dependence of the α-particle energy.

Compared with the yields of ^{76}Br and ^{77}Br taken from the graphically depicted yield functions of Aslam et al. [14] and Hassan and Qaim [15], the deviations of the new data are in very good accordance with the deviant trends in the respective excitation functions. The production rate of ^{76}Br at an α-particle energy of 37 MeV is 24 ± 2 MBq/μA·h and hence about 6 MBq/μA·h higher compared to that reported by Aslam et al. [14] (18 MBq/μA·h) which is connected to the higher maximum cross sections found in this work (see Figure 2). In the case of ^{77}Br the reverse situation is found. Here, the calculated production rate is 23 ± 2 MBq/μA·h and hence about 5 MBq/μA·h lower compared to Hassan and Qaim [15] which again corresponds to the lower cross sections found by the new measurements (see Figure 3). A direct comparison with radionuclide yields published in odler publications is more difficult, due to different conditions ant target materials, like in the case of Alfassi et al. [21], who give a ^{76}Br yield of 155 MBq $\mu A^{-1}h^{-1}$ at 115 MeV α-particle energy calculated from cross section measurements using As

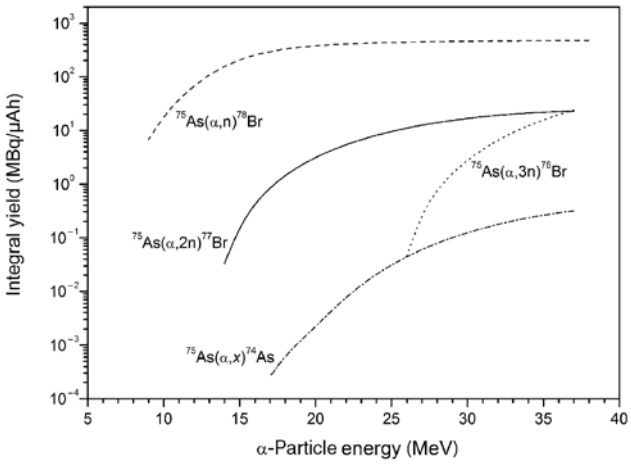

Figure 6: Calculated integral yields of ^{76}Br, ^{77}Br, ^{78}Br and ^{74}As resulting from α-particle induced reactions on arsenic.

powder targets. When checked against the thick target yields given by Dmitriev et al. [33] and Nozaki et al. [20] large deviantions are found. Nozaki et al. determined saturation yields of 2.8 GBq μA^{-1} and 0.91 GBq μA^{-1} of ^{76}Br and ^{77}Br, respectively. Those values accord to about 34.5 MBq $\mu A^{-1}h^{-1}$ of ^{77}Br and 38 MBq $\mu A^{-1}h^{-1}$ of ^{76}Br, being about 50% larger than the new results. Dmitriev et al. [33] reported a ^{76}Br yield of 60.1 MBq $\mu A^{-1}h^{-1}$ and a ^{77}Br yield of 33.9 MBq $\mu A^{-1}h^{-1}$ at an α-particle energy of 43.8 MeV. This large deviantion is also seen in the production yield of ^{74}As reported by Dmitriev and Molin [34] as 0.74 MBq $\mu A^{-1}h^{-1}$, which shows a similar factor of 2.5 to our results. The older result of Blessing et al. however, is lower and corresponds to about 14.4 MBq $\mu A^{-1}h^{-1}$ after normalizing to 100% As as target material. That deviation maybe due to less precise energy calibration pf the α-particle beam.

4 Conclusion

Reaction cross sections of the nuclear reactions ^{75}As(α,*x*n)^{76,77,78}Br and ^{75}As(α,*x*)^{74}As were measured in the energy range up to 38 MeV, and integral yields were calculated with special regard to the production of the medically interesting isotopes ^{76}Br and ^{77}Br. The α-induced reaction does not lend itself to the generation of ^{76}Br for medical application due to the dominant co-production of the longer lived ^{77}Br. The production of ^{77}Br would only be useful in the energy range of 10–37 MeV. Concerning radionuclidic purity, the energy range 17–25 MeV would, however, be most suitable, as the co-production of ^{76}Br is then avoided. Here, the production rate of ^{77}Br is (9.1 ± 0.1) MBq/μA·h, corresponding to a theoretical saturation yield of (1.51 ± 0.02) GBq/μA which was calculated by setting the tenfold half-life of ^{77}Br as irradiation time. Because of its short half-life, the co-production of ^{78}Br is no disadvantage, whereas the non-isotopic radioimpurity ^{74}As can be removed by a suitable chemical separation.

By using the ratios of the monitor nuclides ^{67}Ga/^{66}Ga for the determination of the α-particle energy and the particle flux, the existing nuclear data have been improved. In case of a re-evaluation of the ^{75}As(α,3n)^{76}Br and the ^{75}As(α,2n)^{77}Br reaction, the new cross section data should be taken into account in order to further enhance the accuracy of the corresponding excitation functions.

Acknowledgements: The authors thank very much the cyclotron operator team at VUB involved in the irradiations.

References

1. Maziere, B., Loc'h, C.: Radiopharmaceuticals labeled with bromine isotopes. Appl. Radiat. Isot. **37**, 703 (1986).
2. Rowland, D. J., McCarthy, T. J., Welch, M. J.: Radiobromine for imaging and therapy. In Handbook of Radiopharmaceuticals, John Wiley & Sons, Ltd., Chichester, England (2003), p. 441.
3. Tolmachev, V.; Radiobromine-labelled tracers for positron emission tomography: possibilities and pitfalls. Curr. Radiopharm. **4**, 76 (2011).
4. Coenen, H. H., Moerlein, S. M., Stöcklin, G.: No-carrier-added radiohalogenation methods with heavy halogens. Radiochimica. Acta **34**, 47 (1983).
5. Coenen, H. H.: New radiohalogenation methods: an overview. In: P. H. Cox, S. J. Mather, C. B. Sambson, C. R. Lazarus (Eds.), Progress in Radiopharmacy. Development in Nuclear Medicine 10 Martinus Nijhoff Publishers, Dordrecht (1986), p. 196.
6. Qaim, S. M., Bisinger, T., Hilgers, K., Nayak, D., Coenen, H. H.: Positron emission intensities in the decay of 64Cu, 76Br and 124I. Radiochimica. Acta **95**, 67 (2007).
7. Ribeiro, M. J., Almeida, P., Strul, D., Ferreira, N., Loc'h, C., Brulon, V., Trébossen, R., Mazière, B., Bendriem, B.: Comparison of fluorine-18 and bromine-76 imaging in positron emission tomography. Euro J. Nucl. Med. **26**, 758 (1999).
8. Data extracted using the NNDC On-Line Data Service from the ENSDF database, file revised as of 2014-02-04. Bhat, M. R., Evaluated Nuclear Structure Data File (ENSDF), Nuclear Data for Science and Technology, edited by S. M. Qaim, Berlin, Germany (1992), Springer-Verlag, p. 817.
9. Laforest, R., Liu, X.: Cascade removal and microPET imaging with 76Br. Phy. Med. Biol. **54**, 1503 (2009).
10. Rahmim, A., Zaidi, H.: PET versus SPECT: Strenghts, limitations and challenges. Nucl. Med. Commun. **29**, 193 (2008).
11. Shah, N. J., Herzog, H., Weirich, C., Tellmann, L., Kaffanka, J., Caldeira, L., Rota Kops, E., Qaim, S. M., Coenen, H. H., Iida, H.: Effects of magnetic fields of up to 9.4 T on resolution and contrast of PET images as measured with an MR-brainPET. PLoS One **9**, e95250 (2014).
12. Qaim, S. M., Stöcklin, G.: Production of some medically important short-lived neutron deficient radioisotopes of halogens. Radiochim. Acta **34**, 25 (1983).
13. Qaim, S. M.: Recent developments in the production of 18F, 75,76,77Br and 123I. Appl. Rad. Isot. **37**, 803 (1986).
14. Aslam, M. N., Sudár, S., Hussain, M., Malik, A. A., Qaim, S. M.: Evaluation of excitation functions of proton, 3He- and a-particle induced reactions for production of the medically interesting positron-emitter bromine-76. Appl. Rad. Isot. **69**, 1490 (2011).
15. Hassan, H. E., Qaim, S. M.: A critical survey of experimental cross section data, comparison with nuclear model calculations and estimation of production yields of 77Br and 77Kr in no-carrier-added form via various nuclear processes. Nucl. Instr. Meth. Phys. Res. B, **269**, 1121 (2011).
16. Williamson, C. F., Boujot, J.-P., Picard, J.: Tables of range and stopping power of chemical elements for charged particles of energy 0.05 to 500 MeV. Departement de Physique Nucleaire: Rapport CEA-R 3042 (1966).
17. Tárkányi, F., Takács, S., Gul, K., Hermanne, A., Mustafa, M. G., Nortier, F. M., Oblozinsky, P., Qaim, S. M., Scholten, B., Yu.

Shubin, N., Zhuang, Y.: Beam monitor reactions In: Charged particle cross section database for medical radioisotope production. IAEA-TECDOC-1211, International Atomic Energy Agency, Vienna (2001), p. 49.
18. Piel, H., Qaim, S. M., Stöcklin, G.: Excitation functions of (p,xn)-reactions on natural nickel and highly enriched nickel-62: possibility of production of medically important radioisotope copper-62 at a small cyclotron. Radiochim. Acta **57**, 1 (1992).
19. Kopecky, P.: Proton beam monitoring via the Cu(p,x)58Co, 63Cu(p,2n)62Zn and 65Cu(p,n)65Zn reactions in copper. Int. J. Appl. Radiat. Isot. **36**, 657 (1985).
20. Nozaki, T., Iwamoto, M., Itoh, Y.: Production of 77Br by various nuclear reactions. Appl. Radiat. Isot. **30**, 79 (1979).
21. Alfassi, Z. B., Weinreich, R.: The production of positron emitters 75Br and 76Br: excitation functions and yields for 3He and a-particle induced nuclear reactions on arsenic. Radiochim. Acta **30**, 67 (1982).
22. Paans, A. M. J., Welleweerd, J., Vaalburg, W., Reiffers, S., Woldring, M. G.: Excitation functions for the production of bromine-75: a potential nuclide for the labelling of radiopharmaceuticals. Appl. Radiat. Isot. **31**, 267 (1980).
23. Hermanne, A., Sonck, M., Van Hoyweghen, J., Terriere, D., Mertens, J.: Optimisation of radiobromine production from As-based targets through cross section determination. Proceedings of the International Conference on Nuclear Science and Technology, Gatlinburg, Tennessee (1994) p. 1039.
24. Koning, A. J., Rochman, D., van der Marck, S., Kopecky, J., Sublet, J. C., Pomp, S.: Sjostrand, H., Forrest, R., Bauge, E., Henriksson, H., O. Cabellos, S. Goriely Leppanen, J., Leeb, H., Plompen, A., Mills, R.: TENDL-2014: TALYS-based evaluated nuclear data library. www.talys.eu/tendl-2014.html
25. Kovács, Z., Blessing, G., Qaim, S. M., Stöcklin, G.: Production of 75Br via the 76Se(p,2n)75Br reaction at a compact cyclotron. Appl. Radiat. Isot. **36**, 635 (1985).
26. Hassan, H. E., Qaim, S. M., Shubin, Y., Azzam, A., Morsy, M., Coenen, H. H.: Experimental studies and nuclear model calculations on proton-induced reactions on natSe, 76Se and 77Se with particular reference to the production of the medically interesting radionuclides 76Br and 77Br. Appl. Radiat. Isot. **60**, 899 (2004).
27. Waters, S. L., Nunn, A. D., Thakur, M. L.: Cross-section measurements for the 75As(a,2n)77Br reaction. J. Inorg. Nucl. Chem. **35**, 3413 (1973).
28. Qaim, S. M., Blessing, G., Ollig, H.: Excitation functions of 75As(a,n)78Br and 75As(a,2n)77m,gBr reactions from threshold to 28 MeV. Radiochim. Acta **39**, 57 (1986).
29. Kormány, Z.: A new method and apparatus for measuring the mean energy of cyclotron beams. Nuclear Instruments and Methods in Physics Research Section A: Accelerators, Spectrometers, Detectors and Associated Equipment **337**, 258 (1994).
30. Sudar, S., Qaim, S. M.: Excitation functions of proton and deuteron induced reactions on iron and alpha-particle induced reactions on manganese in the energy region up to 25 Mev. Phys. Rev. **C50**, 2408 (1994).
31. Sudar, S., Qaim, S. M.: Isomeric cross-section ratio for the formation of 58Com,g in neutron, proton, deuteron, and alpha-particle induced reactions in the energy region up to 25 MeV. Phys. Rev. **C53**, 2885 (1996).
32. Levkovskij, V. N.: Activation cross section for the nuclides of medium mass region (A = 40-100) with medium energy (E = 10-50 MeV) protons and alpha-particles (Experiment and Systematics). Inter-Vesti, Moscow, Russia (1991).
33. Dmitriev, P. P., Panarin, M. V., Dmitrieva, Z. B.: Yields of bromine-76, bromine-77, and bromine-82 in nuclear reactions with protons, deuterons, and a-particles. At. En. **52**, 72 (1982).
34. Dmitriev, P. P., Molin, G. A.: Radionuclide yields for thick targets at 22 MeV proton energy. Report Avail. NTIS (1982), (INDC(CCP)-188/L. From: Energy Res. Abstr. Abstr. No. 48059 **8**(19) (1983).